RSC Advances

COMMUNICATION

View Article Online
View Journal | View Issue

Cite this: *RSC Adv.*, 2016, **6**, 91579

Received 9th August 2016
Accepted 16th September 2016

DOI: 10.1039/c6ra20085k

www.rsc.org/advances

# *In situ* synthesis of pristine-graphene/Ag nanocomposites as highly sensitive SERS substrates†

Xiujuan Wang,* Chuhong Zhu,* Zhulin Huang, Xiaoye Hu and Xiaoguang Zhu

In this paper, we proposed a simple *in situ* method for the synthesis of pristine-graphene/Ag nanocomposites by chemical reduction of Ag ions in a *N*-methyl pyrrolidone solution in which pristine-graphene had been homogeneously dispersed. Ag nanoparticles can be directly attached on the pristine-graphene surface without any functionality. The obtained pristine-graphene/Ag nanocomposites are investigated by transmission electron microscopy, X-ray diffraction, and X-ray photoemission spectroscopy. The results show that Ag nanoparticles are homogeneously distributed on the pristine-graphene sheets with high density. We further demonstrate that this pristine-graphene/Ag nanocomposites exhibit a very strong surface-enhanced Raman scattering (SERS) effect, which can be used as ultrasensitive SERS substrates for chemical and biological analysis.

Nanocomposites have attracted wide attention because of their potential to combine the desirable properties of different nanoscale building blocks to improve mechanical, optical, electronic, or magnetic properties.[1–3] Graphene, a single layer of bonded-$sp^2$ carbons compacted into a two-dimensional honeycomb lattice with unique electronic, thermal, and mechanical properties,[4–7] offer new opportunities to develop nanocomposites in many potential applications, ranging from advanced catalytic systems through very sensitive electrochemical sensors to highly efficient fuel cells.[8–15] On the other hand, metal nanoparticles are of great importance due to their optical, catalytic, and electrical properties.[16] It is also a long-term desire to integrate metal nanoparticles into composite materials to explore their properties and applications. Therefore, it is of critical interest if metal nanoparticles can be integrated with graphene to form nanocomposites. However, due to the chemically inert nature of pristine-graphene surface,[17] it is difficult to directly attach metal nanoparticles on the pristine-graphene. Most of the reported methods for the fabrication of graphene/metal nanocomposites are based on the attachment of metal nanoparticles on the graphene oxide (GO) and reduced-GO (rGO).[18–26] Although GO/rGO sheets can be easily dispersed in aqueous solution facilitating the attachment of metal nanoparticles on graphene, it suffers from poor electrical conductivity due to the oxidation-induced defects which disrupt the aromatic system of graphene, limiting its practical applications.[27] Although most of the functional groups in GO can be removed by reduction, large quantities of structural and chemical defects still remain after reduction.[28] Moreover, the electrical conductivity of rGO is only partially restored and lags behind its pristine counterparts.[29] Therefore, to promote technological applications of graphene/metal nanocomposites, new strategies to synthesize high-quality pristine-graphene/metal nanocomposites are indispensable.

In this work, we proposed a simple *in situ* approach for the synthesis of pristine-graphene/Ag nanocomposites by the chemical reduction of Ag ions in the pristine-graphene dispersions in an organic solvent of *N*-methyl pyrrolidone (NMP). By this approach, Ag nanoparticles can be efficiently and uniformly attached on the pristine-graphene with high density. We would like to highlight that it is a facile and efficient process for attaching Ag nanoparticles on pristine-graphene without functionality on the pristine-graphene surface. We further demonstrate that this pristine-graphene/Ag nanocomposites exhibit high surface-enhanced Raman scattering (SERS) activity, which can be used as ultrasensitive SERS platforms for chemical and biological analysis.

The whole preparation strategy for fabricating the pristine-graphene/Ag nanocomposites is shown in Fig. 1. In the first step, the natural graphite was firstly intercalated with concentrated sulfuric acid and hydrogen peroxide to obtain expandable graphite, and then the expandable graphite was rapidly heated at 950 °C for 20 s to obtain expanded graphite. In this process, the natural graphite experiences a sudden and dramatic expansion in the volume due to the decomposition of the intercalating acid of expandable graphite. In the second step,

*Key Laboratory of Materials Physics, and Anhui Key Laboratory of Nanomaterials and Nanotechnology, Institute of Solid State Physics, Chinese Academy of Sciences, Hefei 230031, P. R. China. E-mail: xjwang@issp.ac.cn; chzhu@issp.ac.cn*

† Electronic supplementary information (ESI) available. See DOI: 10.1039/c6ra20085k

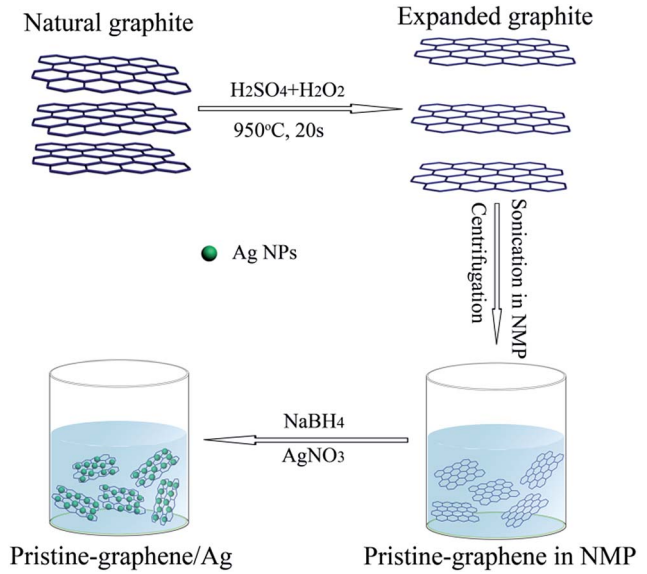


Fig. 1 Schematic illustrations for the synthesis of pristine-graphene/Ag nanocomposites.

the obtained expanded graphite was exfoliated by ultrasonication in NMP solution and then centrifuged to obtain pristine-graphene. In the third step, Ag nanoparticles are deposited on pristine-graphene by chemical reduction of Ag ions with $NaBH_4$ in the pristine-graphene dispersion of NMP.

Fig. 2a and b show scanning electron microscope (SEM) images of the expanded graphite with the "worm-like" structure. The energy required for the layer separation of expanded graphite is much lower than that of natural graphite, thus exfoliation of expanded graphite in NMP could produce higher yields of pristine-graphene compared with the exfoliation of natural graphite in NMP. Fig. 2c shows transmission electron microscopy (TEM) image of the obtained monolayer pristine-graphene with the folded structure, as indicated by the selected area electron diffraction (SAED) pattern (Fig. 2d) taken from the position marked in Fig. 2c.[30] The SAED pattern shows the typical hexagonally arranged lattice of carbon in pristine-graphene, indicating excellent crystallization of the obtained pristine-graphene.[31] The crystal structure of the obtained pristine-graphene was further characterized by Raman spectroscopy (Fig. 3a). The Raman spectrum shows two primary features: a G band at ~1580 $cm^{-1}$ due to the two-fold degenerate E2g mode at the zone centre, and a second-order 2D band at ~2700 $cm^{-1}$ due to phonons in the highest optical branch near the K point at the Brillouin zone boundary.[32] While the disorder-induced modes of D band at 1350 $cm^{-1}$, which relates to the structural defects of graphene, is almost invisible, proving the absence of a significant number of defects in the obtained pristine-graphene.

The high-quality of the obtained pristine-graphene can be further confirmed by X-ray photoelectron spectroscopy (XPS). Fig. 3b shows the XPS spectrum of the obtained pristine-graphene that contains only two peaks of C1s and O1s, which are also apparent in natural graphite. The O peak located at 532.5 eV (Fig. 3c) is assigned to physisorbed $O_2$ or hydrated O species.[33] According to the XPS measurement, the concentration of O atoms in the obtained graphene is 3.49 at%. The high resolution C1s XPS spectrum (Fig. 3d) show only C–C bond with the banding energy of 284.6 eV, while C–O (287.1 eV) and C=O bond (288.8 eV) is almost negligible, further demonstrating the high-quality and absence of oxidization of the obtained pristine-graphene.[34]

The attachment of the Ag nanoparticles on pristine-graphene was characterized by TEM. The typical images of the obtained pristine-graphene/Ag nanocomposites are shown in

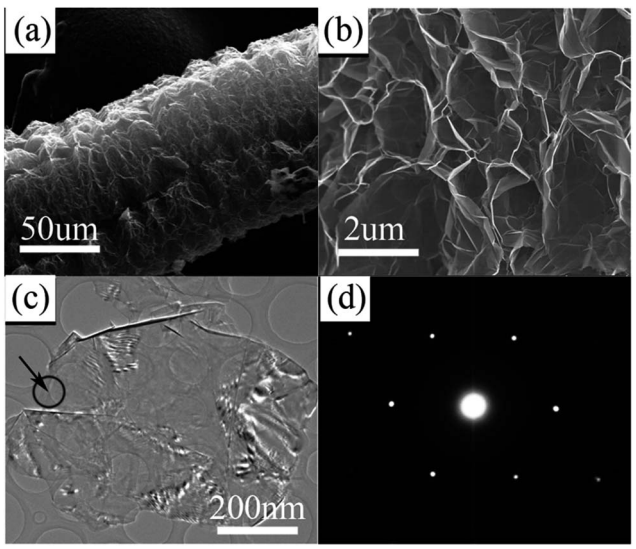


Fig. 2 (a and b) SEM images of the as-synthesized expandable graphite at different magnifications. (c) TEM images of the as-synthesized pristine-graphene sheets (d) electron diffraction pattern for the pristine-graphene sheets, taken from the spot marked in (c).

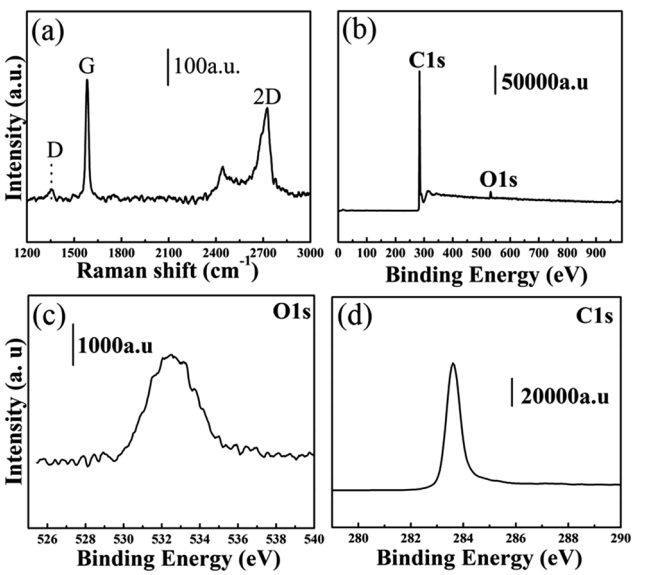


Fig. 3 (a) Raman spectrum, (b) wide-survey scan XPS spectrum, (c) O1s XPS spectrum and (d) C1s XPS spectrum of as-made pristine-graphene.

Fig. 4a and Fig. 4b at different magnifications. It was observed that Ag nanoparticles with a typical diameter of 5–30 nm are homogeneously decorated on the pristine-graphene surface. The distribution of Ag particle size is shown in Fig. S1.† There is no apparent aggregation of Ag nanoparticles on the pristine-graphene, nor large areas of the blank pristine-graphene sheets without Ag nanoparticles decoration. The high resolution TEM (HRTEM) images (Fig. 4c) of Ag nanoparticles indicate that they are single crystals. The measured lattice fringe spacing of 0.23 nm in these Ag nanoparticles corresponds to the (111) crystal plane. The formation of pristine-graphene/Ag nanocomposites was further characterized by X-ray diffraction (XRD) (Fig. 4d), and XPS (Fig. 4e and f). In the XRD diffraction pattern of pristine-graphene/Ag nanocomposites, three of the four main peaks located at 38.4°, 44.3° and 64.5° are assigned to the (111), (200) and (220) planes of cubic Ag crystal, respectively, which indicates that Ag nanoparticles exist in the crystalline state. While the peak located at 26° corresponds to (002) plane of graphite, confirming the high-quality of the obtained pristine-graphene.[35] The XPS spectrum of the obtained pristine-graphene/Ag nanocomposites shows significant Ag 3d signals corresponding to the binding energy of Ag (Fig. 4e), further demonstrating the effective attachment of Ag nanoparticles on the pristine-graphene. In Fig. 4f, it is seen that the C1s spectrum of the pristine-graphene exhibits a sharp peak characteristic of pristine-graphene flakes, the absence of C–O species further confirming the high-quality of the pristine-graphene sheets after attachment of Ag nanoparticles.

SERS can amplify the normal Raman signal by $10^8$ times or more, which has exhibited amazing potential for ultrasensitive analytical applications.[36–38] To achieve ultrasensitive detection of analyte molecules by SERS, the SERS substrate should possess (1) the ability to adsorb enough molecules to contribute to the Raman signal, and (2) abundant nano-scaled gaps known as "hot spots" of noble-metal nanostructures to dramatically enhance the local electromagnetic fields as well as the Raman signal. Based on this knowledge, pristine-graphene/Ag nanocomposites are expected to have high SERS sensitivity with the combined effects of electromagnetic enhancement of Ag nanoparticles[39] and the molecule enricher of graphene.[40] Therefore, to investigate the SERS performance of the obtained pristine-graphene/Ag nanocomposites, Raman measurement was conducted. Fig. 5a shows the Raman spectrum of as-deposited pristine-graphene in the absence of Ag nanoparticles (bottom) in comparison to the spectrum of graphene decorated with Ag nanoparticles (top). Both spectra consist of Raman peaks corresponding to the 1580 $cm^{-1}$ (G band) and 2700 $cm^{-1}$ (2D band), the absence of disorder-induced band at 1350 $cm^{-1}$ for pristine-graphene/Ag nanocomposites demonstrating that the attachment of Ag nanoparticles on the pristine-graphene surface does not introduce any significant defects into the pristine-graphene. As shown in Fig. 5a, a significant enhancement of Raman signals from pristine-graphene/Ag nanocomposites compared to that from pristine-graphene can be observed, which is attribute to the enhancement of the localized electric field at the surface of the Ag nanoparticles in intimate contact with the pristine-graphene.[41] This large Raman enhancement of pristine-graphene by Ag nanoparticles will make the pristine-graphene/Ag nanoparticles system useful as a surface-enhanced Raman scattering platform.

To validate the high SERS sensitivity of the pristine-graphene/Ag nanoparticles hybrid SERS substrates, we used *p*-aminothiophenol (*p*-ATP) molecules, which are commonly used in SERS experiments, to test the SERS performance of the substrates. The SERS spectra of *p*-ATP at different concentrations are shown in Fig. 5b. The peaks located at 1578, 1188, and 1076 $cm^{-1}$ corresponding to $a_1$ vibration modes of *p*-ATP,[42] while the peaks located at 1435, 1391, and 1142 $cm^{-1}$

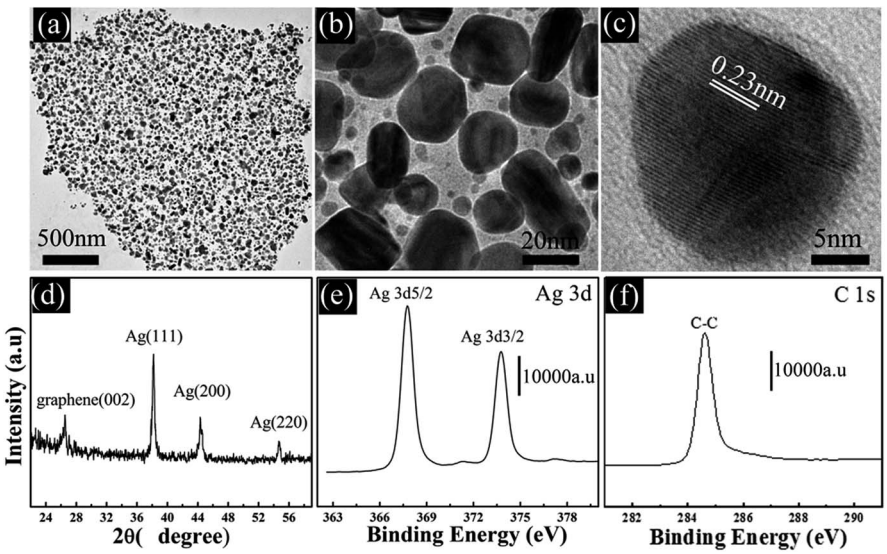


Fig. 4 (a and b) TEM images of the as-synthesized pristine-graphene/Ag nanocomposites at different magnifications. (c) HRTEM image of the Ag nanoparticle. (d) XRD pattern of the pristine-graphene/Ag nanocomposites. (e) XPS spectrum of Ag 3d in the pristine-graphene/Ag nanocomposites. (f) XPS spectrum of C1s in the pristine-graphene/Ag nanocomposites.

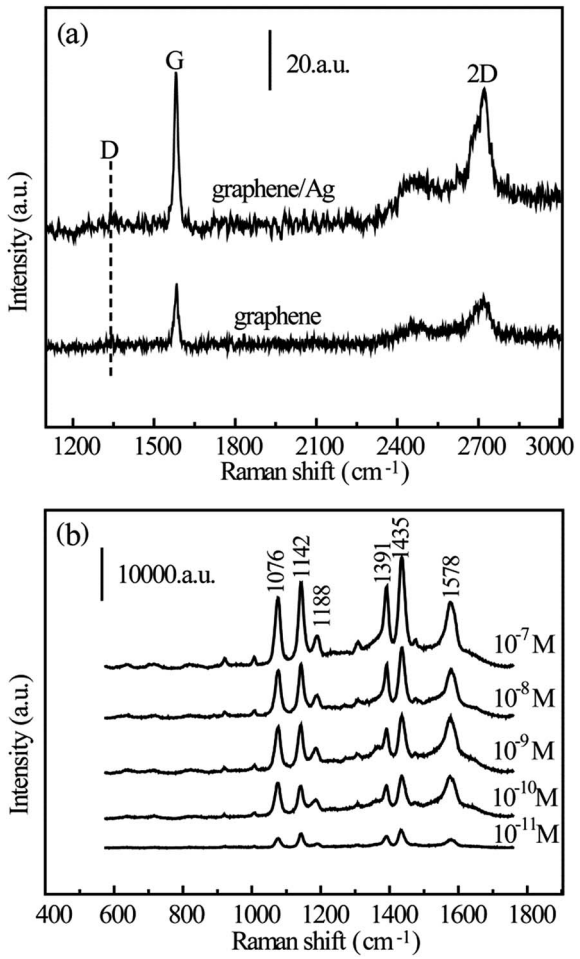


Fig. 5 (a) Raman spectra of the pristine-graphene and the pristine-graphene/Ag nanocomposites. (b) SERS spectra of *p*-ATP at different concentrations on pristine-graphene/Ag nanocomposites.

corresponding to the $a_g$ modes of 4,4′-dimercaptoazobenzene (DMAB) which is an oxidative coupling product of *p*-ATP.[43] According to the report from Xu *et al.*[44,45] the peak at 1142 $cm^{-1}$ attributed to C–H bond, the peaks at 1391 and 1435 $cm^{-1}$ belong to N=N bonds. This result suggests possible chemical transformation of *p*-ATP to DMAB with the laser illumination during SERS measurement.[43–45] It can be seen that the characteristic bands of *p*-ATP are still distinctly observed in the spectra even when the *p*-ATP concentration was down to $10^{-11}$ M, revealing the high SERS sensitivity of the pristine-graphene/Ag nanoparticles hybrid. To further estimate the SERS activity of the pristine-graphene/Ag hybrids, another probe molecule of rhodamine 6G (R6G) was also employed for SERS measurement. Fig. S2† exhibits the dependence of the SERS spectra on the concentration of R6G. Intense SERS spectra were obtained when the concentration of R6G was higher than $10^{-8}$ M. At $10^{-9}$ M, the SERS intensity became much weaker and at the concentration below $10^{-10}$M, Raman signal was hardly detectable. This result shows that the detection limit of R6G reaches as low as $10^{-9}$, further indicating the high SERS sensitivity of the pristine-graphene/Ag nanoparticles hybrid.

# Conclusions

In summary, we have developed a simple *in situ* approach for synthesis of pristine-graphene/Ag nanocomposites by the chemical reduction of Ag ions in the pristine-graphene dispersions in NMP. This approach is of considerable interest as it offers a facile way to directly and uniformly attach high-density Ag nanoparticles on the pristine-graphene without any functionality. The synthesized pristine-graphene/Ag nanocomposites exhibit very strong surface-enhanced Raman scattering SERS effect, which can be used as ultrasensitive SERS substrates for chemical and biological analysis.

# Experimental section

### Materials

All common reagents and solvents were purchased from the Shanghai Chemical Factory (Shanghai, China) and used as received without further purification. Natural graphite was purchased from Qingdao Hensen Graphite Co., Ltd. Water used throughout all experiments was purified with the Millipore system.

### Preparation of pristine-graphene

First, the natural graphite was mixed with a mixture (20 : 1 by volume) of concentrated sulfuric acid (98 wt%) and hydrogen peroxide (30 wt%). The obtained mixture was then stirred for about 1 h and then washed with deionized water until the pH level reached 5. After drying at 100 °C for 24 h, the expandable graphite was obtained. Then the obtained expandable graphite was rapidly heated at 950 °C for 20 s in Ar atmosphere to produce expanded graphite. After that, the expanded graphite was dispersed in the NMP at a concentration of 0.1 mg $L^{-1}$ by sonication for 40 min. The resultant dispersion was then centrifuged at 1000 rpm for 10 min. The top half of the graphene dispersion was collected for further use.

### Synthesis of pristine-graphene/Ag nanocomposites

0.02 g PVP ($M_w \sim 55\,000$) was dispersed into 20 mL pristine-graphene NMP dispersion by rapid stirring. Then 1 mL $AgNO_3$ (0.5 M) and 1 mL $NaBH_4$ (0.5 M) were added to the above solution in sequence under vigorous stirring. The resulting solution was stirred for 1 h at room temperature. Finally, the obtained stable black dispersion was centrifuged and washed three times with ethanol and then dissolved in 20 mL ethanol.

### Characterization of pristine-graphene/metal-NPs hybrids

TEM measurements were made on a HITACHI H-8100 EM with an accelerating voltage of 200 kV. For TEM observation, carbon-coated copper grids were dipped in pristine-graphene/metal-nanoparticles solution and then dried in ambient conditions. The XPS measurements were carried out using a VG ESCALAB 220i-XL system, equipped with a monochromatized Al Kα source ($h\nu$ = 1486.6 eV) for the excitation of photoelectrons. XRD patterns were recorded using a Bruker D8 Advance X-ray diffractometer with Cu-Kα radiation.

 

**Raman measurements**

Raman spectra were obtained by using a confocal microprobe Raman system (Renishaw, inVia) with an excitation wavelength of 532 nm. To ensure good molecule adsorption, the as-synthesized pristine-graphene/AgNPs hybrids spin-coated on Si substrate were immersed in 1.5 mL *p*-ATP aqueous solutions (from $10^{-7}$ to $10^{-11}$ M) for 12 h, taken out and then dried in air. All the spectra were acquired with the acquisition time of 5 s.

## Acknowledgements

This work was financially supported by the National Key Basic Research Program of China (Grant 2013CB934304), and the Natural Science Foundation of China (Grants 21577146, 61006068, and 21201168).

## Notes and references

1 V. Georgakilas, D. Gournis, V. Tzitzios, L. Pasquato, D. M. Guldi and M. Pratodf, *J. Mater. Chem.*, 2007, **17**, 2679.
2 X. H. Peng, J. Y. Chen, J. A. Misewich and S. S. Wong, *Chem. Soc. Rev.*, 2009, **38**, 1076.
3 S. J. Guo and S. J. Dong, *Chem. Soc. Rev.*, 2011, **40**, 2644.
4 K. S. Novoselov, A. K. Geim, S. V. Morozov, D. Jiang, Y. Zhang, S. V. Dubonos, I. V. Grigorieva and A. A. Firsov, *Science*, 2004, **306**, 666.
5 A. K. Geim, *Science*, 2009, **324**, 1530.
6 R. R. Nair, P. Blake, A. N. Grigorenko, K. S. Novoselov, T. J. Booth, T. Stauber, N. M. R. Peres and A. K. Geim, *Science*, 2008, **320**, 1308.
7 C. Lee, X. D. Wei and J. W. Kysar, *Science*, 2008, **321**, 385–388.
8 J. Liu, S. Fu, B. Yuan, Y. Li and Z. Deng, *J. Am. Chem. Soc.*, 2010, **132**, 7279.
9 S. Yang, X. Feng, L. Wang, K. Tang, J. Maier and K. Mullen, *Angew. Chem., Int. Ed.*, 2010, **49**, 4795.
10 D. H. Lee, J. E. Kim, T. H. Han, J. W. Hwang, S. Jeon, S.-Y. Choi, S. H. Hong, W. J. Lee, R. S. Ruo and S. O. Kim, *Adv. Mater.*, 2010, **22**, 1247.
11 K. E. Byun, D. S. Choi, E. Kim, D. H. Seo, H. Yang, S. Seo and S. H. Hong, *ACS Nano*, 2011, **5**, 8656.
12 Z. P. Song, T. Xu, M. L. Gordin, Y. B. Jiang, I. T. Bae, Q. F. Xiao, H. Zhan, J. Liu and D. H. Wang, *Nano Lett.*, 2012, **12**, 2205.
13 U. J. Kim, I. H. Lee, J. J. Bae, S. Lee, G. H. Han, S. J. Chae, F. Günes, J. H. Choi, C. W. Baik, S. Kim, J. M. Kim and Y. H. Lee, *Adv. Mater.*, 2011, **23**, 3809.
14 S. M. Paek, E. Yoo and I. Honma, *Nano Lett.*, 2009, **9**, 72–75.
15 H. J. Zhang, P. P. Xu, G. D. Du, Z. W. Chen, K. K. Oh, D. Y. Pan and Z. Jiao, *Nano Res.*, 2011, **4**, 274.
16 G. Hodes, *Adv. Mater.*, 2007, **19**, 639.
17 O. C. Compton and S. T. Nguyen, *Small*, 2010, **6**, 711.
18 J. F. Shen, M. Shi, N. Li, B. Yan, H. W. Ma, Y. Z. Hu and M. X. Ye, *Nano Res.*, 2010, **3**, 339.
19 R. Pasricha, S. Gupta and A. K. Srivastava, *Small*, 2009, **5**, 2253.
20 W. Ren, Y. X. Fang and E. K. Wang, *ACS Nano*, 2011, **5**, 6425.
21 K. Jasuja and V. Berry, *ACS Nano*, 2009, **3**, 2358.
22 R. J. Liu, S. W. Li, X. L. Yu, G. J. Zhang, S. L. Zhang, J. N. Yao, B. Keita, L. Nadjo and L. J. Zhi, *Small*, 2012, **8**, 1398.
23 A. Mastalir, Z. Kiraly, A. Patzko and P. LArgentiere, *Carbon*, 2008, **46**, 1631.
24 G. M. Scheuermann, L. Rumi, P. Steurer, W. Bannwarth and R. Mulhaupt, *J. Am. Chem. Soc.*, 2009, **131**, 8262.
25 E. Yoo, T. Okata, T. Akita, M. Kohyama, J. Nakamura and I. Honma, *Nano Lett.*, 2009, **9**, 2255.
26 Y. G. Zhou, J. J. Chen, F. B. Wang, Z. H. Sheng and X. H. Xia, *Chem. Commun.*, 2010, **46**, 5951.
27 S. Stankovich, D. A. Dikin, R. D. Piner, K. A. Kohlhaas, A. Kleinhammes, Y. Jia, Y. Wu, S. T. Nguyen and R. S. Ruoff, *Carbon*, 2007, **45**, 1558.
28 G. Eda, G. Fanchini and M. Chhowalla, *Nat. Nanotechnol.*, 2008, **3**, 270.
29 C. Gomez-Navarro, R. T. Weitz, A. M. Bittner, M. Scolari, A. Mews, M. Burghard and K. Kern, *Nano Lett.*, 2007, **7**, 3499.
30 Y. Hernandez, V. Nicolosi, M. Lotya, F. M. Blighe, Z. Sun, S. De, I. T. McGovern, B. Holland, M. Byrne, Y. K. Gun'Ko, J. J. Boland, P. Niraj, G. Duesberg, S. Krishnamurthy, R. Goodhue, J. Hutchison, V. Scardaci, A. C. Ferrari and J. N. Coleman, *Nat. Nanotechnol.*, 2008, **3**, 563.
31 J. C. Meyer, A. K. Geim, M. I. Katsnelson, K. S. Novoselov, T. J. Booth and S. Roth, *Nature*, 2007, **446**, 60.
32 A. C. Ferrari, J. C. Meyer, V. Scardaci, C. Casiraghi, M. Lazzeri, F. Mauri, S. Piscanec, D. Jiang, K. S. Novoselov, S. Roth and A. K. Geim, *Phys. Rev. Lett.*, 2006, **97**, 187401.
33 M.-H. Cho, D.-H. Ko, K. Jeong, S. W. Whangbo, C. N. Whang, S. C. Choi and S. J. Cho, *Thin Solid Films*, 1999, **349**, 266.
34 X. L. Li, G. Y. Zhang, X. D. Bai, X. M. Sun, X. R. Wang, E. Wang and H. J. Dai, *Nat. Nanotechnol.*, 2008, **3**, 538.
35 Z. Q. Li, C. J. Lu, Z. P. Xia, Y. Zhou and Z. Luo, *Carbon*, 2007, **45**, 1686.
36 M. Fleischmann, P. J. Hendra and A. J. McQuillan, *Chem. Phys. Lett.*, 1974, **26**, 163.
37 M. G. Albrecht and J. A. Creighton, *J. Am. Chem. Soc.*, 1977, **99**, 5215.
38 D. L. Jeanmaire and R. P. Van Duyne, *J. Electroanal. Chem.*, 1977, **84**, 1.
39 M. Rycenga, C. M. Cobley, J. Zeng, W. Li, C. H. Moran, Q. Zhang, D. Qin and Y. Xia, *Chem. Rev.*, 2011, **111**, 3669.
40 W. Ren, Y. X. Fang and E. K. Wang, *ACS Nano*, 2011, **5**, 6425.
41 A. N. Sidorov, G. W. Sławinski, A. H. Jayatissa, F. P. amborini and G. U. Sumanasekera, *Carbon*, 2012, **50**, 699.
42 M. Osawa, N. K. Matsuda, K. Yoshii and I. Uchida, *J. Phys. Chem.*, 1994, **98**, 12702.
43 Y. F. Huang, H. P. Zhu, G. K. Liu, D. Y. Wu, B. Ren and Z. Q. Tian, *J. Am. Chem. Soc.*, 2010, **132**, 92.
44 J. Y. Chu, P. Miao, X. J. Han, Y. C. Du, X. J. Wang, B. Song and P. Xu, *ChemCatChem*, 2016, **8**, 1.
45 P. Xu, L. L. Kang, N. H. Mack, K. S. Schanze, X. J. Han and H. L. Wang, *Sci. Rep.*, 2013, **2013**(3), 2997.